Electronic Supplementary Material (ESI) for Biomaterials Science.

Investigation and Comparison of resin materials in transparent DLP-printing for application in cell culture and Organs-on-a-Chip

Anna Fritschen[1], Alena K. Bell[2], Inga Königstein[1], Lukas Stühn[2], Robert W. Stark[2], Andreas Blaeser[1,3]

[1]Technical University of Darmstadt, Department of Mechanical Engineering, BioMedical Printing Technology, Magdalenenstr. 2, 64289 Darmstadt, Germany
[2]Technical University of Darmstadt, Institute of Materials Science, Physics of Surfaces, Alarich-Weiss-Str. 10, 64287 Darmstadt, Germany.
[3]Technical University of Darmstadt, Centre for Synthetic Biology, Schnittspahnstr. 10, 64287 Darmstadt, Germany

Supporting Information

1. UV/VIS spectrophotometry of resins

UV/VIS spectrophotometry (300 nm to 800 nm) of all resins and the components for the PEG-DA based resins reveals that all materials are transparent above 400 nm. Differences arise between 300 to 400 nm. The absorbance properties of the photo initiator and photo sensitizer govern the spectrum for PEG-DA based resins (Figure S1).

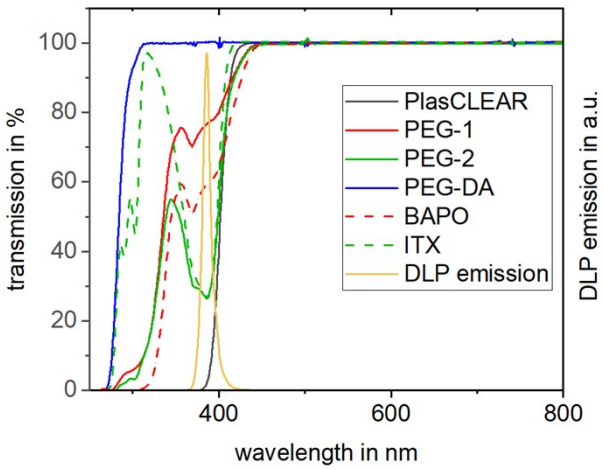

Figure S1: UV/VIS spectra of resins and their components compared to the DLP emission spectrum in the wavelength range from 300 nm to 800 nm. The ready-to-use liquid resins are shown in continuous black (PlasCLEAR), red (PEG-1), and green (PEG-2) lines, the liquid PEG-DA with a continuous blue line and the DLP emission spectrum in a continuous yellow line. The photo initiator (BAPO) is represented with a dashed red line and the photo sensitizer (ITX) with a dashed green line.

2. Raman overview spectra of PEG-DA based resins

Raman overview spectra of PEG-DA based materials show a high fluorescence signal at wavenumbers from 300 to 1500 cm^{-1} for parts with no UV exposure after printing. The fluorescence signal vanished with increasing UV exposure (Figure 13).

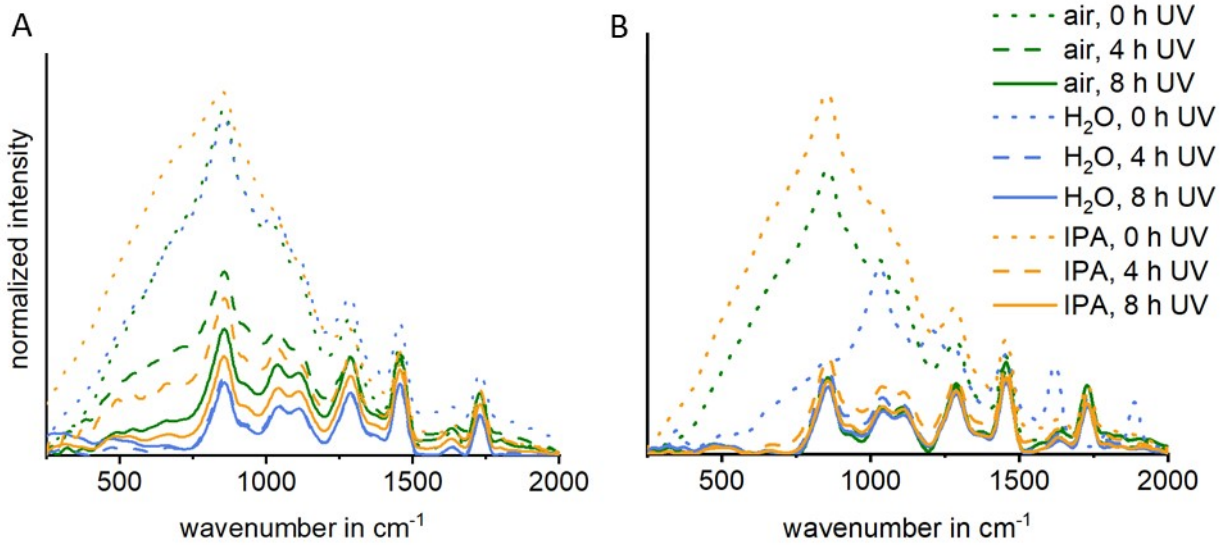

Figure S2: Raman overview spectra on printed PEG-1 (A) and PEG-2 (B) parts showing Raman fluorescence for parts with no UV exposure. The colors represent the different overnight extraction media (air in green, water in blue, IPA in red) and the line types show the UV exposure time (0 h dotted line, 4 h dashed line, 8 h solid line) in the respective color.

3. Transmission spectra of printed parts

The UV/VIS spectra of printed parts depending on post-treatment (overnight extraction medium and UV exposure time) are given in Figure S3. The data of PlasCLEAR samples (Figure S3 A) show no influence of the post treatment. PEG-1 data (Figure S3 B) show a dent (360 nm-380 nm) before UV exposure which vanishes with UV treatment. This dent appears in the spectrum due to the photo initiator BAPO. The data of PEG-2 (Figure S3 C) show two dents due to photo initiator (BAPO, maximum at 360 nm) and photo sensitizer (ITX, maximum at 380 nm). Both vanish with increasing UV exposure time.

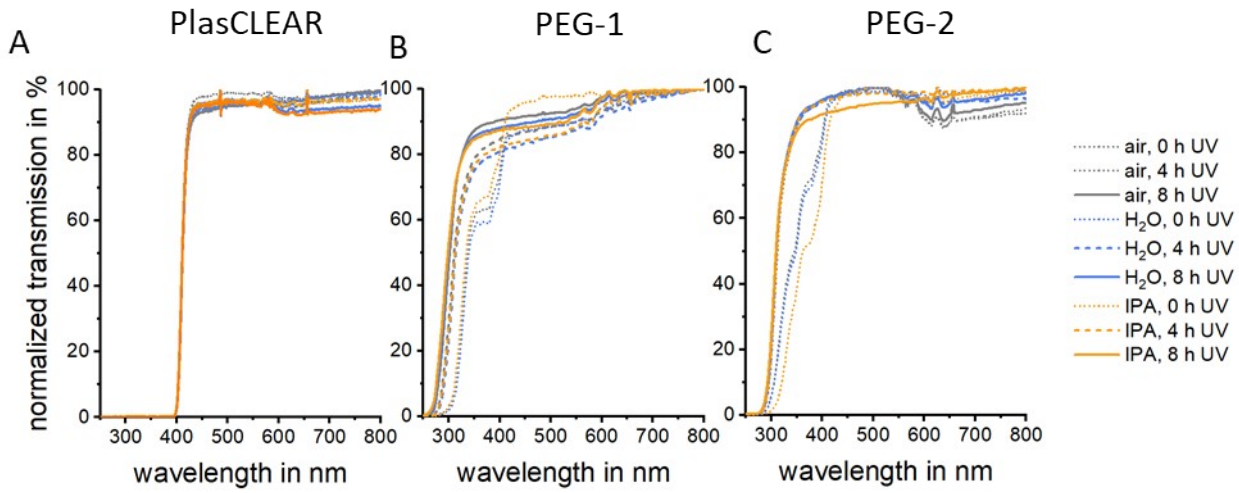

Figure S3: Normalized transmission spectra obtained by UV/VIS spectrophotometry of PlasCLEAR (A), PEG-1 (B) and PEG-2 (C) printed parts with different post-treatments steps. Extraction medium (black, blue, and orange lines) and UV exposure time (dotted, dashed, and solid linetypes) are given.

4. Fluorescence microscopy of HUVECs on printed parts in dependence on post-treatment

Fluorescence microscopy images were taken of HUVECs cultivated on transparently printed cell culture dishes. Prints were plasma treated before cell seeding. Actin filaments were stained with Alexa Fluor 488-phalloidin and cell nuclei with DAPI. Images are shown for post-treatment combinations where cells attached and proliferated, otherwise no images are included (Figure S4 – S6). Biocompatibility and cell viability depend on the extraction medium for PlasCLEAR parts and on the UV exposure time for the PEG-DA based resins.

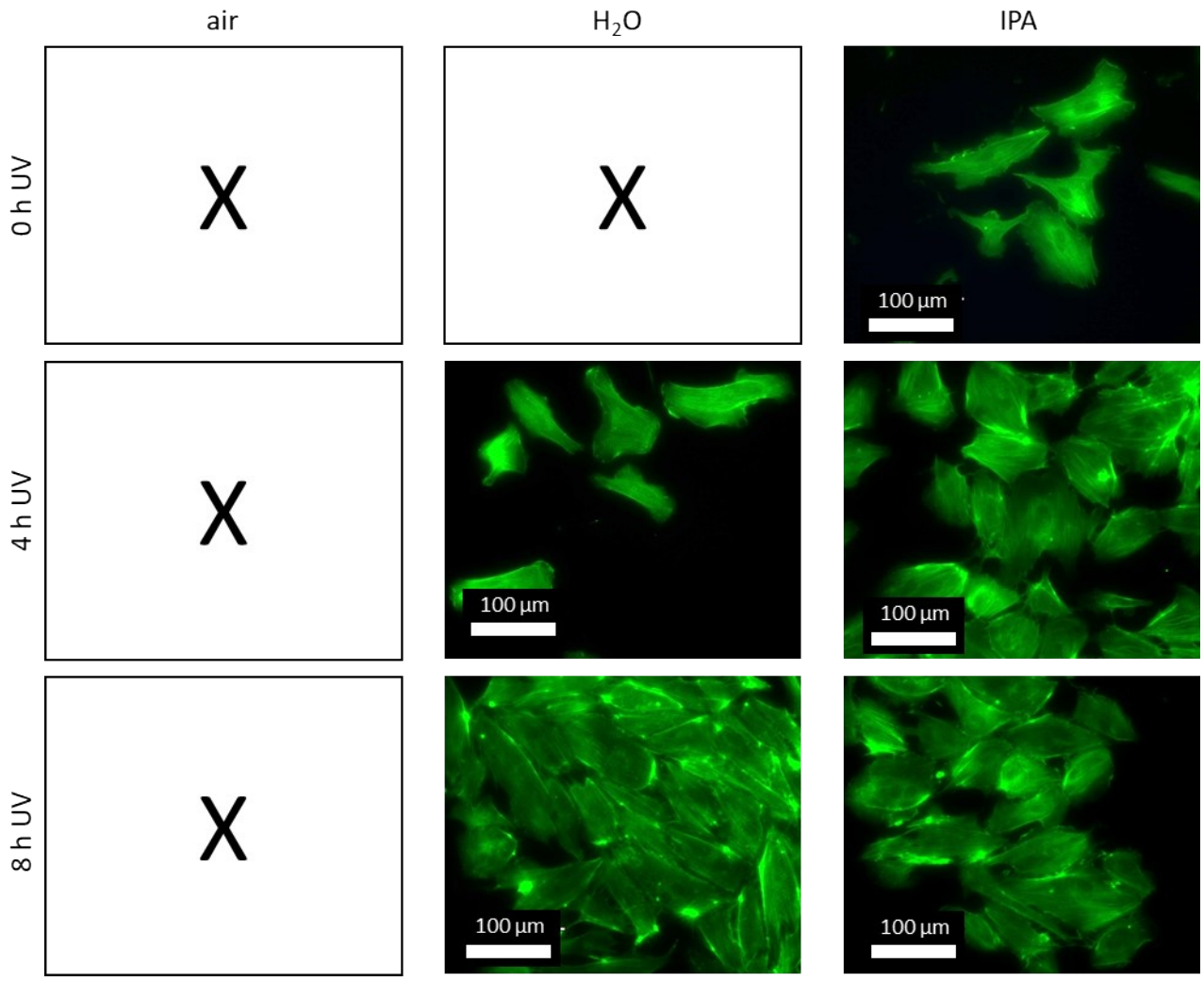

Figure S4: Fluorescence microscopy of HUVECs cultured on PlasCLEAR printed parts with different post-treatment combinations of extraction medium and UV exposure time. Actin filaments were stained with Alexa Fluor 488-phalloidin (green). On post-treatment variations marked with X no cells attached onto parts.

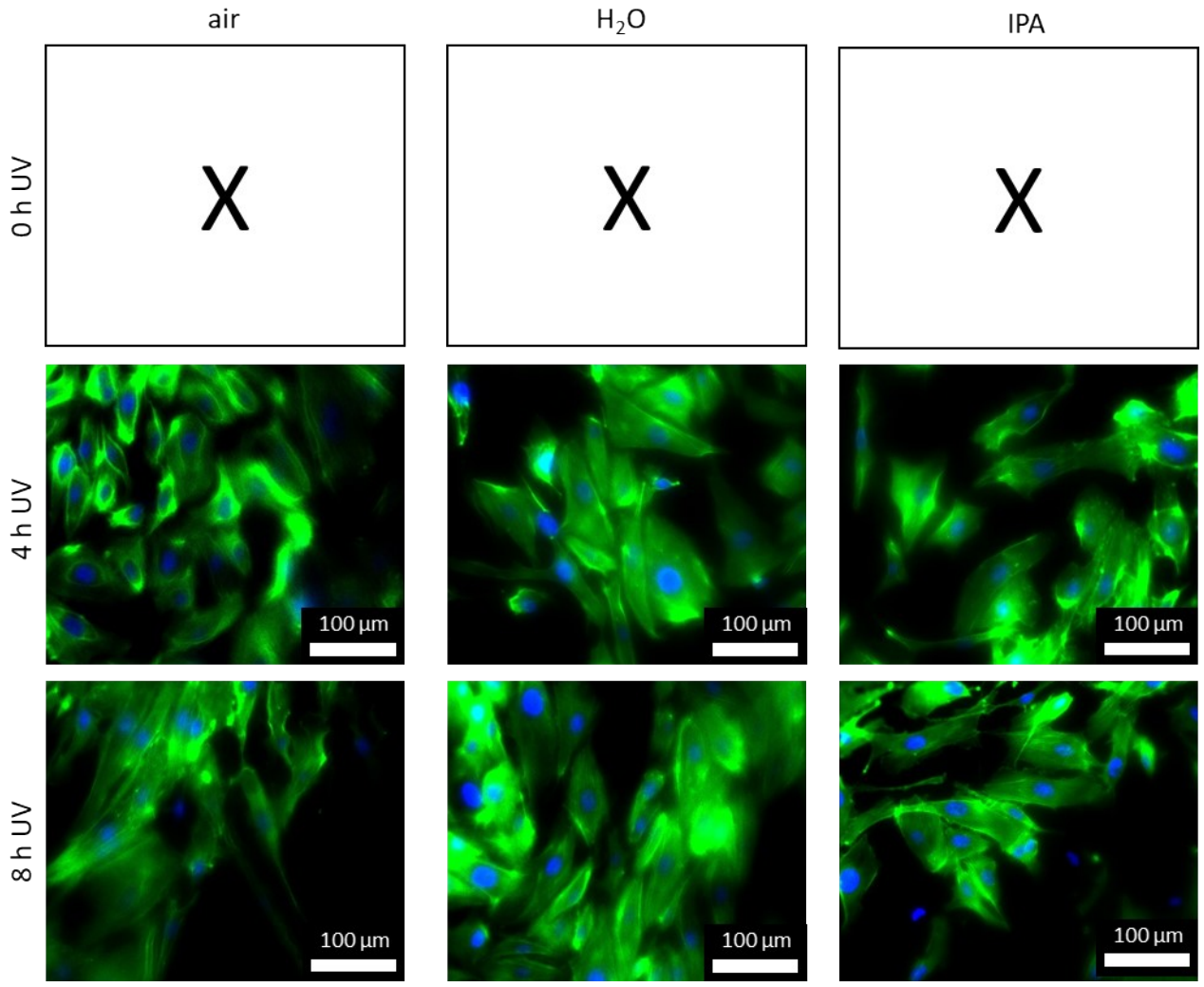

Figure S5: Fluorescence microscopy of HUVECs cultured on PEG-1 printed parts with different post-treatment combinations of extraction medium and UV exposure time. Actin filaments were stained with Alexa Fluor 488-phalloidin (green) and cell nuclei with DAPI (blue). On post-treatment variations marked with X no cells attached onto parts.

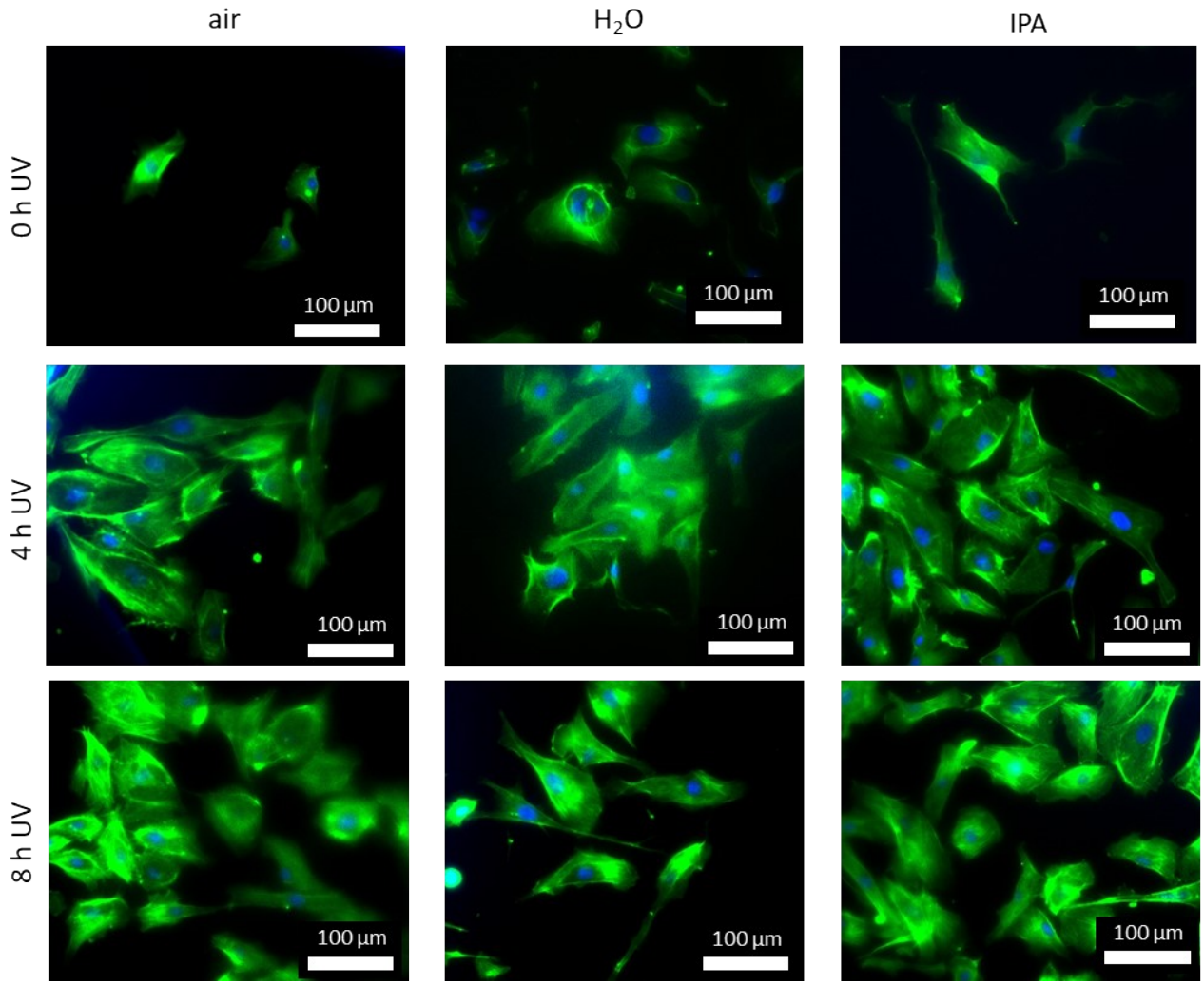

Figure S6: Fluorescence microscopy of HUVECs cultured on PEG-2 printed parts with different post-treatment combinations of extraction medium and UV exposure time. Actin filaments were stained with Alexa Fluor 488-phalloidin (green) and cell nuclei with DAPI (blue). On post-treatment variations marked with X no cells attached onto parts.

5. Light microscopy of L929 fibroblasts on printed parts

L929 fibroblasts were cultured on printed parts and studied under a light microscope (Figure S6). Images reveal the good optical properties of prints under phase contrast as well as fluorescence microscopy at up to 400 times magnification. The cells' nuclei were stained with DAPI (blue) and actin filaments with Alexa Fluor 488-phalloidin (green). For cells cultured on PlasCLEAR, the DAPI staining is not visible as the parts absorb the excitation wavelength of light as shown in UV/VIS measurements (Figure 5, main manuscript).

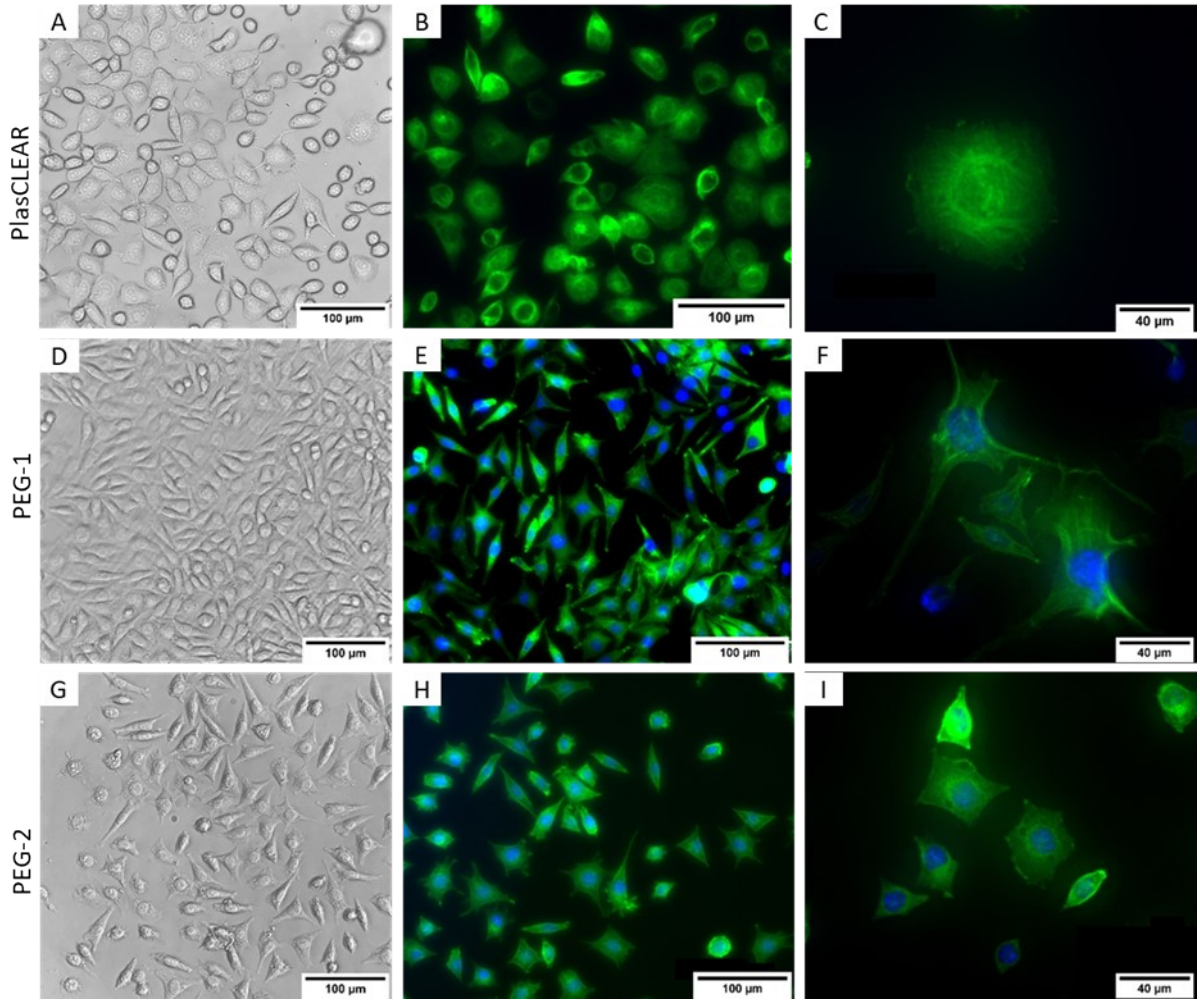

Figure S7: Light microscopy imaging of L929 mouse fibroblasts cultured on printed parts. Phase contrast and fluorescence microscopy images of L929 stained with DAPI (blue) for cell nuclei and Alexa Fluor 488-phalloidin (green) for actin filaments at two magnifications.

6. Atomic force microscopy measurements of surface topography

Peak-Force tapping atomic force microscopy (AFM) measurements of the surfaces of printed parts reveal that the printer's DLP mirrors are reproduced as surface features as observed in light microscopy (Figure 7, main manuscript). Periodic height variations occur over a width of 27 µm, which equals the DLP pixel size of the printer (Figure S7 bottom). The height deviations are small (40 nm) for PlasCLEAR and PEG-1, but amplified by the factor 10 (up to 400 nm) for PEG-2. This demonstrates the impact of the photo sensitizer on the localization of the cross linking reaction, which is also present for printing small features.

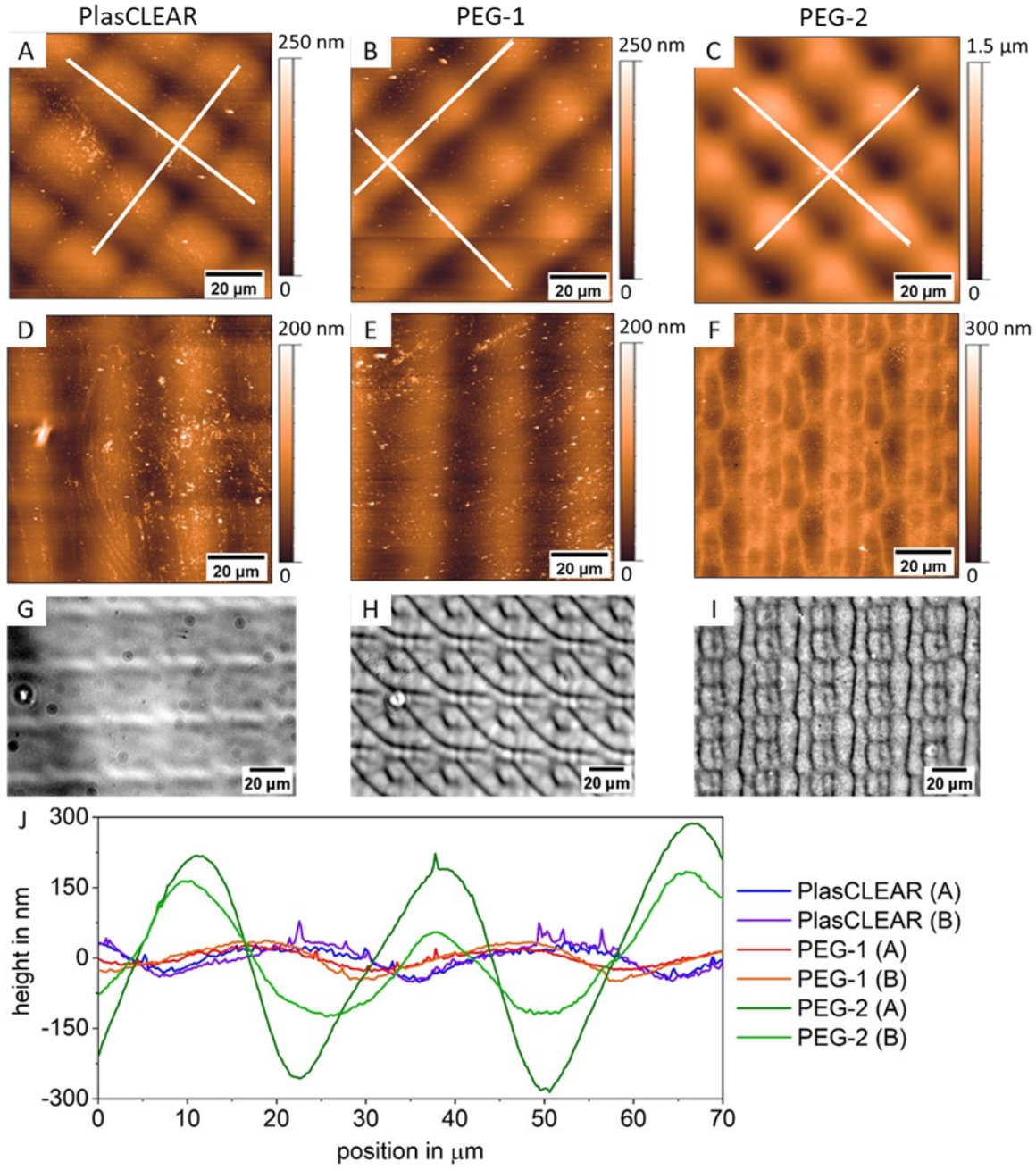

Figure S8: Peak force tapping AFM images on printed parts taken at a 45° angle to DLP pixels (A-C) and in line with DLP pixels (D-F), where the line flattening function of the AFM software removes the height differences in scan direction. Phase contrast images show the influence of height deviations during light microscopy (G-I). Two height profiles along the indicated lines in A-C for each material reveal higher height deviation for PEG-2 (J).

7. Design of Experiment results

A screening design of experiment (DoE) was conducted to identify the print parameters with the greatest influence on pillars and holes. For PlasCLEAR, the DoE included 8 print parameters, which was reduced to 4 for PEG-1 and PEG-2. For all materials, light intensity and exposure time at a certain slice thickness showed the greatest effect in the analyzed parameter ranges. For pillars, an increase in light intensity and exposure time, therefore an increasing energy input, had a negative effect on print quality (Figure 11 A-C), which means that the deviation of the designed diameter compared to the measured diameter of the prints decreased and the accuracy of prints improved. This was the opposite for holes, where a higher energy input led to overcuring and therefore to a higher deviation of the measured hole diameter compared to the targeted value (Figure 11 D-F).

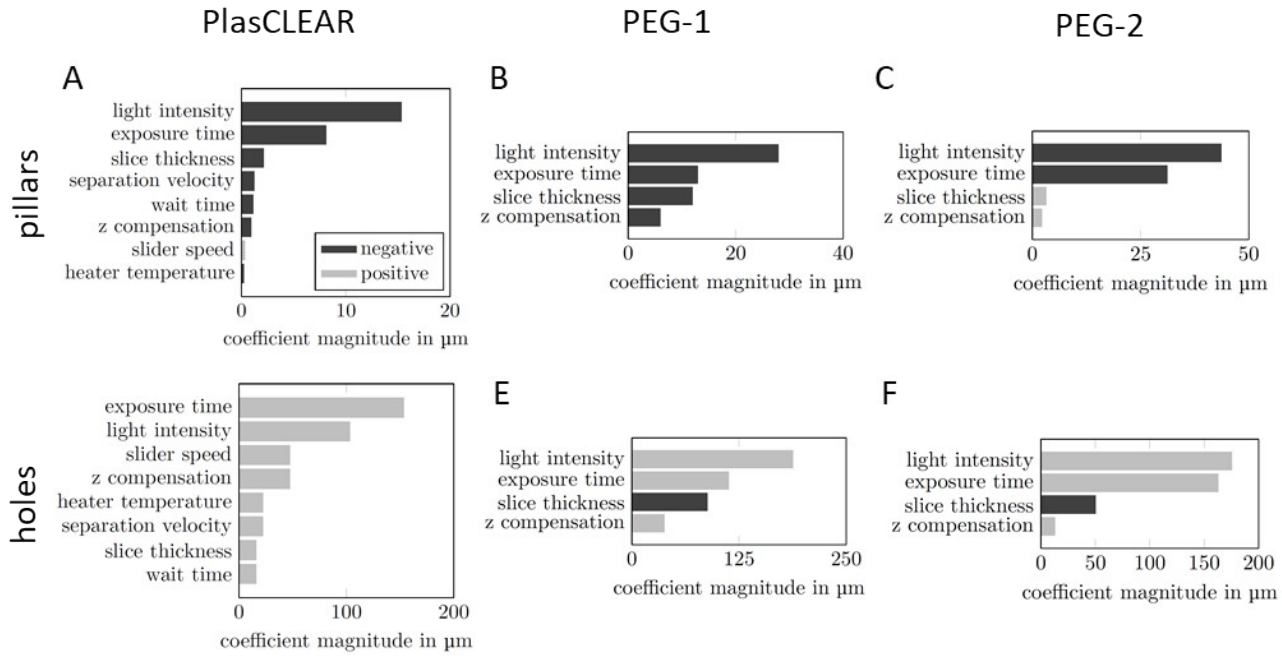

Figure S9: Results of a DoE screening show the magnitude of effect of the examined print parameters on the resolution of prints for PlasCLEAR (A,D), PEG-1 (B,E) and PEG-2 (C,F). Output variables were the deviation of the pillar diameter from the target (A-C) and the smallest hole being sufficiently open (D-F).